

## MULTILAYERS ACTIVITIES AT SACLAY / ORSAY

C. Baumier<sup>1,2,3</sup>, C.Z. Antoine<sup>3</sup>, F. Fortuna<sup>2</sup>, G. Martinet<sup>1</sup>, J.-C. Villegier<sup>4</sup>,  
<sup>1</sup> IPNO, IN2P3-CNRS, Université Paris Sud 11, F-91406 Orsay Cedex, France  
<sup>2</sup> CSNSM IN2P3-CNRS, Université Paris Sud 11, F-91406 Orsay Cedex, France  
<sup>3</sup> CEA, Irfu, SACM, Centre d'Etudes de Saclay, 91191 Gif-sur-Yvette Cedex, France  
<sup>4</sup> CEA, Inac, 17 Rue des Martyrs, 38054 Grenoble-Cedex-9, France

### Abstract

In the investigations on the high gradient SRF cavities, the superconducting multilayer is a promising alternative. The predictions show that SIS nanocomposite (Superconductor/Isolator/Superconductor) could improve the efficiency limited by the bulk Nb it-self used today for accelerating cavities. We started, at the IPNO lab in collaboration with the CSNSM lab (CNRS) and Irfu lab (CEA), an experimental study to test the screening effect on multilayer assemblies. Based on 3<sup>rd</sup> harmonic magnetometer and a TE011 SRF cavity, measurements of first critical magnetic field  $H_{C1}$  and surface resistance of samples have been performed. These promising results are the starting point of the MBE deposition developments. This setup is devoted to optimize the best organization of the multilayer to produce the model sample, and to find, in a close future, a realistic solution to apply this technique on an accelerating SRF cavity.

### INTRODUCTION

Bulk Niobium has held the monopoly for the fabrication of high  $Q_0$ , high accelerating gradient RF cavities for accelerators over 3 decades.

Record accelerating gradient are close to 40-45 mV/m (TESLA shape), corresponding to a magnetic component of the RF field close to 200mT near the surface of the cavity. For many years the ultimate limits of RF cavities, based on the superheating model were nevertheless expected to reach higher fields (55-65 MV/m). Years of active R&D did not allow pushing Niobium toward higher field and the applicability of superheating model in practical conditions (high field, high duty cycle, low temperature) is questioned.

Indeed even in his famous paper, Yogi noticed that far from  $T_C$ , individual vortices could enter the material faster than the RF period [1].

It is now established that individual vortices can enter the material in less than  $10^{-13}$  sec and that surface defect can promote vortices penetration [2-4].

There are also several theoretical and experimental evidences that nonlinear BCS resistance and vortex penetration can be the source of thermal dissipation in superconducting cavities [2, 5-8].

Early vortex penetration at surface defects could also explain the monopoly of Niobium in SRF applications since Nb has the highest  $H_{C1}$  value (180 mT at 0 K) among all superconductors: high  $H_{C1}$  material is mandatory to prevent bulk vortex penetration even if the

surface  $H_{C1}$  is deprived by surface defects (asperities, grains boundaries...).

Attempts to use higher  $T_C$  and  $H_{C2}$  superconductors have failed so far, probably due to their low  $H_{C1}$ .

### MULTILAYERS

Very high  $H_{C1}$  can indeed be achieved with films whose thickness  $d$  is smaller than the magnetic penetration depth  $\lambda$ : the field is attenuated by screening currents but for energetic reason it is not possible to nucleate a vortex in such thin film. A. Gurevich proposed to use such films to screen bulk Niobium and allow much higher field to be reached inside cavities [9]. Several layers are needed to efficiently damp the external field, separated by an insulating layer to prevent Josephson coupling between each layer.

Depositing such nanometric composite structure will be a complex issue, but the deposition of model samples with asserted techniques used to build similar structures (Magnetron Sputtering, Molecular Beam Epitaxy) will allow to better understand their physical properties, and hopefully find an optimization route.

### EXPERIMENTAL DETAILS

#### *Samples Description*

- SL: one 25 nm single NbN layer on the top of one 14 nm MgO deposited on a 250 nm Nb layer.
- R is the same sample as SL but with the top NbN layer removed by RIE etching to provide a single Niobium reference.
- ML4 is a set of four MgO (14 nm)/NbN (25 nm) layers deposited onto 500 nm of Nb on sapphire. A bulk RRR 300 Niobium disc (for RF cavity measurement) was also deposited in the same conditions. (sample rf-ML4) The surface of the Nb disk was simply chemically etched before deposition of the multilayer coating and the surface roughness was not optimized (see Figure 1 and Table 1).
- rf-ML2 is a bulk Large Grain Niobium (RRR 300) disk deposited with set of two MgO(14 nm)/NbN (50 nm), so that the total thickness of NbN is the same as ML4.
- rf-Nb is a bulk RRR 300 Nb disk.

All these characteristics are summarized in table 1.

Table I: Samples characteristics

Samples	Niobium thickness	Number of NbN/MgO <sup>a</sup> sequences	T <sub>c</sub> (K)
R	250 nm	0	8.9 <sup>b</sup>
SL	250 nm	1x 25 nm	16.38 <sup>b</sup>
ML4a	500 nm	4x 25 nm	15.1 <sup>c</sup>
rf-ML4	bulk, PX	4x 25 nm	
rf-ML2	bulk LG	2 x50nm	Not known
rf-Nb	bulk, PX	0	

PX: polycrystalline; LG : large grain

a. For all samples: intermediate MgO thickness is 14 nm). SL and MLs are covered with a last 5nm MgO capping.

b. Measured with a Quantum Design PPMS®.

c. Measured with local magnetometry at low field.

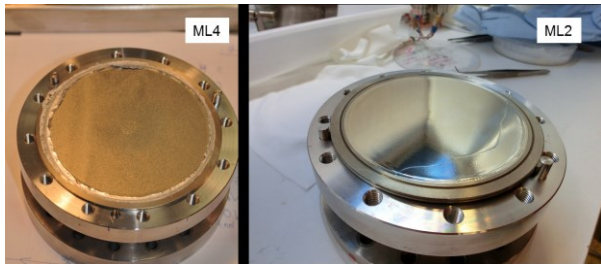


Figure 1: Samples rf-ML4 (polycrystalline Nb) and rf-ML2 (LG). Pitting due to the Nb substrate etching can still be observed underneath the nanometric layers. Rf-ML2 exhibits also a clear grain boundary between the two main grains of the surface.

### 3rd Harmonic Analysis

The third harmonic local magnetometer principle [10, 11] is based on the fact that when a coil is small enough compare to the sample size, then the sample can be considered like an infinite plane (due to field attenuation with distance). When the sample is in the Meissner state and current is applied into the coil, the sample acts like a perfect magnetic mirror, and the coil behaves linearly. Then the temperature is slowly increased, when it reaches the transition temperature at the actual field seen by the sample, vortices start entering and pinning in the sample. Pinned vortices produce a “dragging forces” on the electrons coil and its behavior is not linear anymore. The coil being parallel to the surface, no Bean-Livingston barrier is expected. The temperature where a 3<sup>rd</sup> harmonic signal appears for various field is thus actually the signature of the first critical field  $H_{C1}$ .

Measurements on single and multilayers deposited on Niobium have been published elsewhere [12-16], at field limited below 60 mT. On Figure 2, one can clearly see that at higher field, the signal is not the expected Gaussian curve, but reflects the interference between the various films of the multilayer.

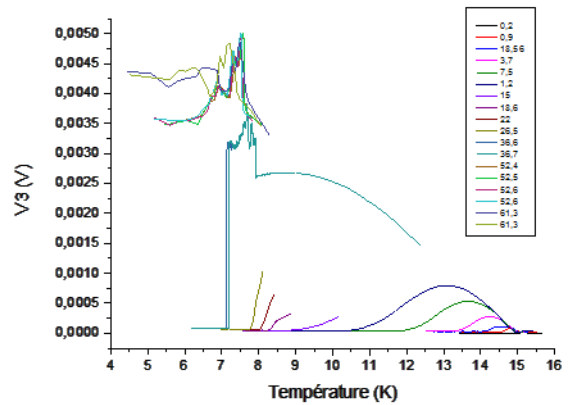


Figure 2: Series of measurement for the ML4 sample. Corresponding field are listed in the legend box (in mT).

Recently we have improved the thermal design of the experimental set-up and were able to characterize samples up to 150 mT over large temperature ranges.

In particular we have re-tested the sample ML4 over a wider temperature range, and discovered that the transition previously observed in [12] were in fact sitting on the top of a broader transition that dramatically occurs between 36 and 38 mT (see Figure 2).

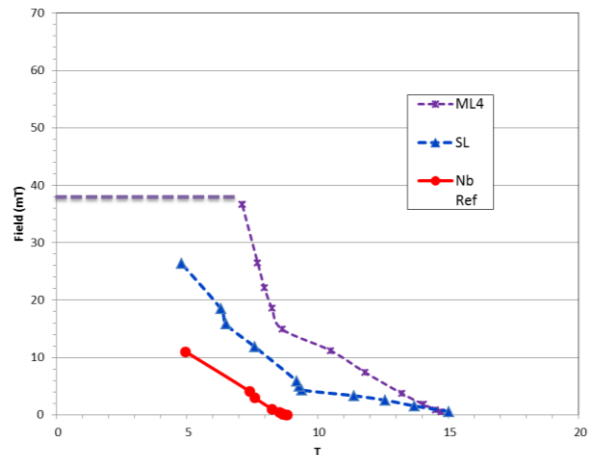


Figure 3: Measurement of the transition of various single and multilayer samples.

The transition is so abrupt it can probably be attributed to the fact the field lines have surrounded the sample. At high field, with a sample with 1 cm radius compared to the coil diameter (2.5 mm), the condition  $R_{\text{sample}} \gg R_{\text{coil}}$  is no longer valid (Figure 3). Although these results are somewhat less good than was initially hoped, ML4 exhibit a transition field  $\sim 30$  mT higher than sputtered Niobium, confirming the screening effect of only 100 nm of NbN total thickness. Hopefully, the future use of thicker samples should help us to confirm this trend.

In order to check the effect of thicker layers, a samples was deposited on a large grain niobium disc for RF

testing with 2x50 nm of NbN ( $H_{C1}$  will be measured soon on a cutoff).

**RF TE011 Characterization**

TE011 cavity is a tool of choice for testing flat samples deposited with standard deposition technique, and later on with techniques more adapted to accelerating cavities with more complex shape.

TE011 cavity has a fundamental mode at 3.88 GHz where the magnetic field is ring shaped and maximum at the bottom of the feed-through, at the intersection with the top of the cavity but no field on the edges. The TE012 mode at 5.12 GHz presents the same type of field repartition (Figure 4). The use of two frequencies gives access to the frequency dependence of the surface resistance of the samples.

This field repartition allows placing a removable flat sample (13 cm diameter) at the top of the cavity, with negligible field on the indium seal that makes the cavity vacuum tight.

The other advantage of this configuration is the absence of perpendicular electric field on the surface which renders the cavity insensitive to dust contamination (no field emission). If handled with care, no clean room assembly is necessary.

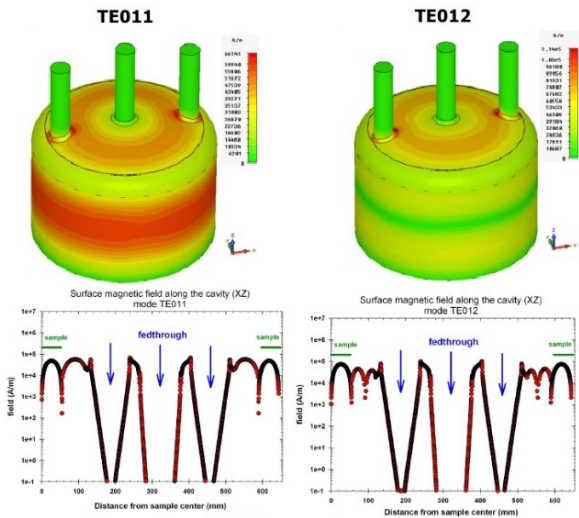


Figure 4: field repartition for the TE011 et TE012 modes.

Figure 5 shows the raw RF data for rf-Nb and rf-ML2 samples.

The contribution of the surface resistance from the samples to the whole cavity  $Q_0$  is coarsely 20%. Indeed not much difference is observed in the two sets of curves (Nb vs ML2) from Figure 5. One important conclusion can be drawn from these results: the residual resistance from the multilayer is very high. Indeed, the residual resistance is the only unpredictable part of surface resistance, and a high  $R_{res}$  like the one found in e.g. HTSC would have seriously preclude the whole ML concept.

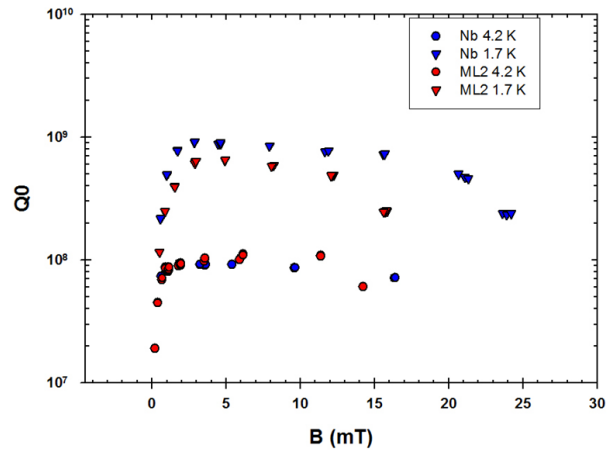


Figure 5: Raw RF data at 4.2 and 1.7 K for rf-Nb and rf-ML2 samples. The two sets of curves are very similar showing that the sample does not influence much the overall cavity's behavior.

The thermometric system attached to the sample allows having a more precise idea of the surface resistance of the sample independently of the cavity body.

The backside of sample is held under vacuum, except its 3 mm thick edge, in contact with the helium bath that ensures sample cooling. This configuration allows up to 150 mW dissipation at 1.5 K for bulk niobium and 10 times more if the substrate is copper. In the vacuum chamber a system of thermal sensors and a calibrated resistance allows determining the thermal behavior of the sample: the thermometers are mounted on the backside of the sample and are encapsulated in copper to improve thermal contact with the sample. The contact is maintained by bronze-beryllium springs. 3 lines of 6 thermometers forming an angle of 120° between each other allow measuring the temperature profile from the center to the border of the sample. Six other thermometer pairs are mounted near the edge of the disk. A calibrated heater is fixed on the center of the disk to calibrate both the thermometers and the dissipated power from the sample [17].

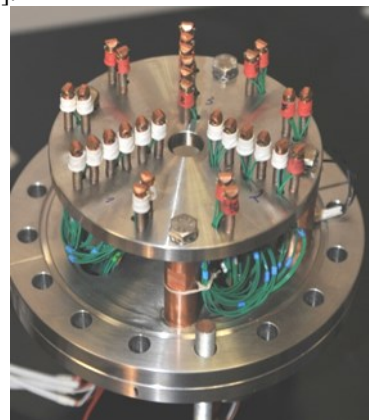


Figure 6: repartition of thermal sensors and the calibrated heater on the backside of the sample.

This system allows in a first stage to measure its thermal behavior of the sample in the presence of a known power deposition (calibrated resistance), and then in the second stage, to measure the final temperature profile with RF field applied on sample which is correlated to the dissipated power on the surface of the sample.

The surface resistance is calculated using:

$$P_{dis.} = \frac{1}{2} \iint R_S \cdot H_S^2 dS \quad (1)$$

where  $P_{dis.}$  is the dissipated power on the surface sample,  $R_S$  the surface resistance and  $H_S$  the surface magnetic field.

Due to the thermometer distribution, 9 different sectors of the sample can be independently measured, which renders the information redundant but helps to discriminate the behavior of a local defect from the overall sample behavior.

Figure 7 shows the surface resistance the samples rf-ML4 for a surface magnetic field of 1 mT, compared with a good 1.3 GHz, scaled with  $\omega^2$  law. This scaling is probably not fully correct for the residual part of  $R_S$ , but is acknowledged for the BCS part of the surface resistance  $R_{BCS}$  [3]. On the same plot we have also indicated the results of rf-ML2 and rf-Nb at 4,2 and 1.7 K. At low temperature (residual resistance regime), sample rf-ML4, deposited on a rough polycrystalline Nb disc, obviously exhibit a higher surface resistance Nb (about 3 times higher than rf- Nb and 10 times than scaled Nb), whereas rf-ML2 deposited on a smooth large grain material compares to Nb. This support the idea that residual resistance will not be the main obstacle for the development of multilayers, and that room for improvement can be found.

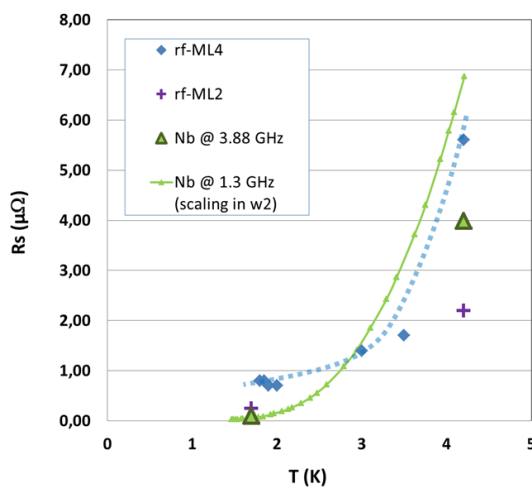


Figure 7: RF surface resistance of Nb, rf-ML2 and rf-ML4 measured at 3.88 GHz. For sake of comparison, the surface resistance of a good 1.3 GHz cavity is also shown, scaled with an  $\omega^2$  law.

At higher temperature (BCS regime), ML samples seems to behave better than Nb. In particular the measurement of rf-Nb and rf-ML2 done with the same calibration at 4,2 K show a significant factor 2 in favor to multilayers.

With a total thickness of 100 nm of NbN, and assuming  $\lambda \sim 200$  nm for NbN, the respective contributions to the surface resistance of the nanometric layers and niobium are of the same order of magnitude (cf Equation (1)):

$$\tilde{R}_S = (1 - e^{-2L/\lambda})R_{ML} + e^{-2L/\lambda}R_{Nb} \quad (2)$$

Where  $L$  is the NbN layer thickness,  $\lambda$  its penetration depth and  $R_{ML}$  its BCS surface resistance of NbN.  $R_{NB}$  stands for the BCS resistance of bulk niobium.

The observed result is consistent with part of the screening current flooding in the NbN layers with  $T_C$  close to 17 K and a surface resistance  $\sim 1/10$  of that of bulk niobium [4].

Several routes of improvement can already be foreseen:

- One can expect that with more or thicker layers, the contribution of bulk Nb would become negligible.
- Influence of the interface between the Nb matrix and the multilayers must be studied and the surface preparation of the niobium must be improved accordingly.

## MBE

We need to determine how the screening properties evolve in more realistic situations. We plan to test samples deposited on bulk monocrystalline and polycrystalline Niobium. The preparation of multiple samples requires the development of a home deposition set-up. In this context we are now upgrading an existing MBE set-up from CSNSM.

The choice of MBE: MBE is known to be able to grow very pure layers, with a controlled thickness and crystallographic properties (depending on the substrate).

The existing set-up was able to deposit any pure element (including Nb and Mg...). The adjunction of a RF source to the system is necessary to be able to prepare nitride starting from a bulk metal source.

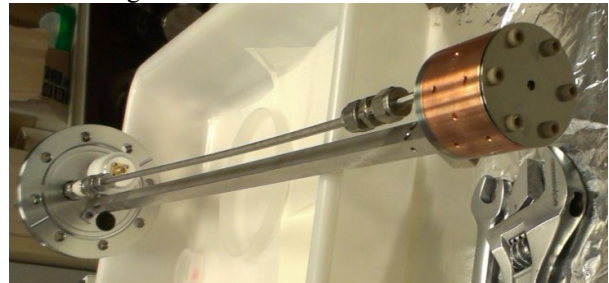


Figure 8: Special UHV adapted COMICS source to provide nitrogen molecular beam. Niobium beam is provided by a secondary atomic source in the same experimental set-up.

We have chosen to adapt a special source (COMICS sources) developed initially at LPSC (Grenoble). These sources have the advantage of being very compact and

adaptable to different elements like nitrogen in this case, but any other gas like oxygen could be used. We have extended this concept to ultrahigh vacuum (as needed in MBE).

The source is now under commissioning.

## PERSPECTIVES AND CONCLUSION

We have presented the superconducting properties of composite structures specifically designed for RF accelerating applications. ML structures seem to be a promising way to go beyond Nb for accelerator cavities, providing effective screening of the surface, preventing early vortex penetration and  $R_{BCS}$  improvement thanks to the use of higher  $T_C$  superconductors.

The important information is that  $R_{res}$  is the same order of magnitude as Nb. Indeed in the multilayer model there was no way to predict this part of surface resistance. A very high residual resistance would have seriously impeded the concept.

A better understanding of interaction with substrate is needed to improve these layers performances.

Two strategies need to be developed in parallel:

- Deposition method for cavities (not treated in this paper).
- Understanding the physics of ML and optimization of their structures.

Adequate tools for the testing of many samples are now effective. Effort must be now carried on the production of ML on samples and cavities.

## ACKNOWLEDGEMENTS

The research leading to these results has received partial funding from the European Commission under the FP7 Research Infrastructures project EuCARD2, grant agreement no. 227579.

The project has received a partial funding from P2IO-LaBex as well.

For the mechanical realization: A special thanks to Mr. H. Ringuenet, Mr. P. Leroy, and Mr. B. Pilette.

## REFERENCES

- [1] T. Yogi, G. Dick, and J. Mercereau, "Critical rf magnetic fields for some type-I and type-II superconductors". *Physical Review Letters*, 1977. **39**(13): p. 826-829.
- [2] A. Gurevich and G. Ciovati, "Dynamics of vortex penetration, jumpwise instabilities, and nonlinear surface resistance of type-II superconductors in strong rf fields". *Physical Review B* 2008. **77**(10): p. 104501-21.
- [3] E.H. Brandt. "Electrodynamics of superconductors exposed to high frequency fields". in International workshop on thin films and new ideas for pushing the limit of RF superconductivity. 2006. Legnaro National Laboratories (Padua) ITALY.
- [4] D.Y. Vodolazov, "Effect of surface defects on the first field for vortex entry in type-II superconductors". *Physical Review B*, 2000. **62**(13): p. 8691.
- [5] A. Gurevich, "Multiscale mechanisms of SRF breakdown". *Physica C*, 2006. **441**(1-2): p. 38-43
- [6] T. Proslir, et al., "Localized magnetism on the surface of niobium: experiments and theory". *Bulletin of the American Physical Society*, 2011. **56**.
- [7] G. Ciovati and A. Gurevich. "Measurement of RF losses due to trapped flux in large-grain niobium cavity". in SRF 2007. 2008. Beijing, China: Thomas Jefferson National Accelerator Facility, Newport News, VA.
- [8] G. Ciovati and A. Gurevich, "Evidence of high-field radio-frequency hot spots due to trapped vortices in niobium cavities". *Physical Review Special Topics-Accelerators and Beams*, 2008. **11**(12): p. 122001.
- [9] A. Gurevich, "Enhancement of RF breakdown field of SC by multilayer coating". *Appl. Phys.Lett.*, 2006. **88**: p. 012511.
- [10] G. Lamura, et al., "First critical field measurements by third harmonic analysis ". *Journal of Applied Physics*, 2009. **106**: p. 053903.
- [11] M. Aurino, et al., "Discrete model analysis of the critical current-density measurements in superconducting thin films by a single-coil inductive method". *Journal of Applied Physics*, 2005. **98**: p. 123901.
- [12] C.Z. Antoine, J.C. Villegier, and G. Martinet, "Study of nanometric superconducting multilayers for magnetic field screening applications". *Applied Physics Letters*, 2013. **102**(10): p. 102603.
- [13] C.Z. Antoine, et al. "Magnetic screening of NbN multilayers samples". in SRF 2011. 2011. Chicago, IL, USA.
- [14] C.Z. Antoine, et al., "Characterization of field penetration in superconducting multilayers samples". *IEEE Transactions on Applied Superconductivity*, 2011. **21** (3): p. 2601 - 2604.
- [15] C.Z. Antoine, et al., "Characterization of superconducting nanometric multilayer samples for SRF applications: first evidence of magnetic screening effect". *Physical Review Special Topics-Accelerators and Beams*, 2010. **13**: p. 121001.
- [16] C.Z. Antoine, et al. "Characterization of superconducting multilayer samples". in SRF 2009. 2009. Berlin, Germany.
- [17] G. Martinet, et al. "Development of a TE011 Cavity for Thin-Films Study". in SRF 2009. 2009. Berlin.